Ostwald ripening in a semi-infinite system

R. Burghaus
Institut für Theoretische Physik IV, Heinrich-Heine-Universität Düsseldorf, Universitätsstrasse 1, D-40225 Düsseldorf, Germany
(Received 12 September 1997)

The Ostwald ripening of droplets in a supersaturated vapor is analyzed in a semi-infinite system bounded by an unwetted wall. Whereas in an unbounded system only the growth of the droplet radius is taken into account, the distance of the droplet from the wall enters as a second dynamic variable in a semi-infinite system. In the space of these two variables the ripening process is described by a set of trajectories that display a depletion layer of about three critical radii in thickness above the boundary wall. The asymptotic droplet-number distribution is also calculated as a function of the two variables. [S1063-651X(98)10503-2]

PACS number(s): 64.60.Qb, 64.60.My, 64.75.+g

The dynamics of phase separation in bulk systems is a well-studied subject [1,2]. Recently, interest has shifted to the influence of walls on, e.g., nucleation [3–5] and spinodal decomposition [6–11] where mainly the early stages have been considered. In the present work the late-stage growth of nucleation-induced Ostwald ripening in a semi-infinite system is discussed. Ostwald ripening is the process of phase separation in a supersaturated binary mixture by diffusional growth of supercritical nuclei of the minority phase. In a fluid system at low initial supersaturation spherical droplets will typically be nucleated at large mutual separation so that the diffusional droplet growth can be described in a single-droplet picture. In the Lifshitz-Slyozov-Wagner (LSW) theory of Ostwald ripening [12–14] in an infinite system the droplet growth is coupled to the concentration field to obey global mass conservation. The main results of this theory are the overall growth rate of the minority phase and, moreover, the droplet number density distribution at the late stage, which turns out to be independent of the details of the initial nucleation process.

In the following we consider a semi-infinite system with a dry boundary wall. Extending the standard LSW theory for an infinite system, the distance z of the droplet center from the wall will be taken as a second dynamic quantity in addition to the droplet radius a. Under the assumption of slow diffusion, the concentration field surrounding a spherical droplet becomes quasistationary so that the corresponding diffusion equation reduces to the Laplace equation. The concentration along the droplet surface c_s is determined by the Gibbs-Thomson relation

$$c_s(a)=c_0\left(1+\Lambda\frac{2}{a}\right), \tag{1}$$

where c_0 is the concentration above a planar condensate and Λ is a capillary length. In order to solve this diffusion problem, we use an electrostatic analogy where the droplet is replaced by a conducting sphere. Then the concentration field, multiplied with the diffusion constant D, resembles the electric field surrounding the sphere, also with Dirichlet boundary conditions. The volume growth rate $\dot{V}$ of the droplet (i.e., the total flux into the droplet) corresponds to 4π times the charge of the conductor. Since this charge is given by the capacity C times the potential difference to infinity, we conclude that

$$\dot{V}(a)=4\pi DC(a,z)[c_\infty-c_s(a)]. \tag{2}$$

Together with Eq. (1) this shows that $a_{\rm cr}=2\Lambda c_0/(c_\infty-c_0)$ is the critical radius of the droplet. The normal derivative of the concentration field at the boundary wall of the system vanishes because there is no diffusion flux into the wall. This Neumann boundary condition is implicitly fulfilled, if the method of mirror charges is used with the wall taken as the reflection surface. In this way the growth properties of a droplet are described by the electrostatics of a capacitor consisting of two spheres with a spacing of $2z$ between their centers. The capacity of one of these spheres is [15]

$$C(a,z)=a\ \sinh(\mu)\sum_{s=1}^{\infty}(-1)^{s+1}\sinh(s\mu)^{-1},$$
$$z/a\equiv\cosh(\mu). \tag{3}$$

C converges to the bulk value $C=a$ for $(z/a)\to\infty$ and decreases monotonically for $(z/a)\to1$ because of the reduced diffusion flux screened by the wall. Also, the presence of the wall gives rise to an anisotropy of the diffusion-flux density along the surface of the growing droplet. Assuming that the hydrodynamic relaxation of the droplet shape is fast compared to the diffusional growth, the droplet remains spherical but has an effective drift perpendicular to the wall due to the above-mentioned screening effect. The drift is calculated by integration of the diffusion-flux density times the distance from the droplet center of mass along the droplet surface divided by its mass. This leads to

$$\dot{z}=3\,D(c_\infty-c_s(a))\frac{\sinh(\mu)}{a}\sum_{s=1}^{\infty}(-1)^{s+1}\frac{\sinh(s\mu)}{\sinh^2[(s+1)\mu]}, \tag{4}$$

where the expression for the diffusion-flux density has been adopted from the result for the charge density of a capacitor [15]. The z drift vanishes far away from the wall (as in an infinite system) but increases when the distance to the wall is diminished.

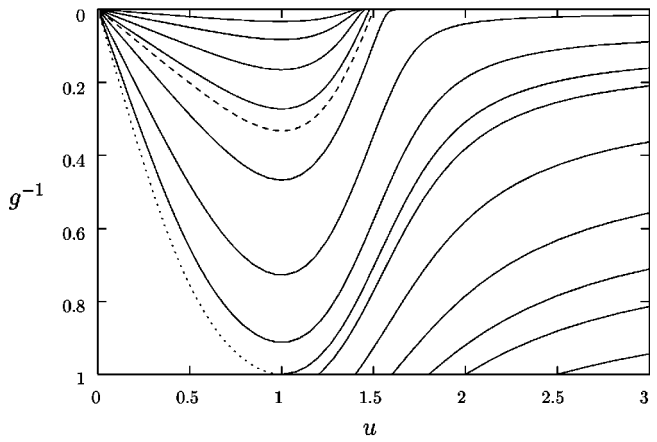

FIG. 1. Trajectories $g^{-1}(u)$.

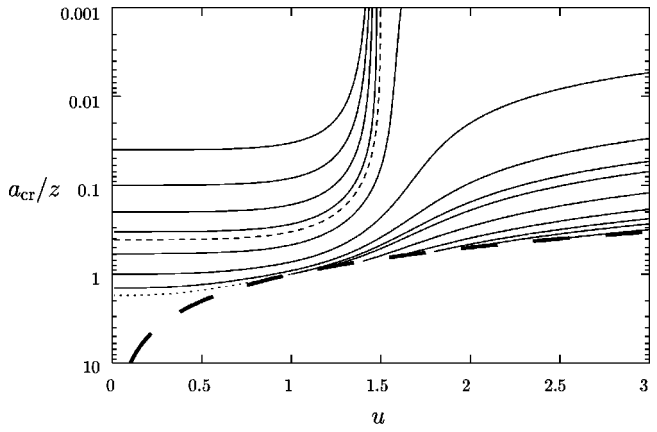

FIG. 2. Trajectories $a_{cr}(u)/z$. The thick long-dashed line marks the droplet in contact with the wall ($g=1$).

A dry wall in contact with a supersaturated system turns out to be stable if the droplets nucleated on the wall are spherical caps with contact angles $\theta > \pi/2$ [16]. The growth rate for the curvature radius of such a droplet can also be calculated using the electrostatic analogy. In this case the mirror image of the droplet is a symmetric bispherical lens. The result $\dot{a}$ is identical to that of a spherical droplet in the bulk except for a constant prefactor $k(\theta)$ with $k(\theta)<1$ for $\theta > \pi/2$ [16,17]. Therefore the radii of supercritical nuclei on the wall get surpassed by the critical radius, which is driven by the faster growth of the droplets in the volume [16]. Consequently, the droplets on the wall shrink so that the wall eventually becomes dry.

For the discussion of an ensemble of droplets in the bulk the single droplet growth rates will be written in dimensionless units following the procedure of Lifshitz and Slyozov [12,13]. In terms of the dimensionless variables $u = a/a_{cr}(t)$, $g = z/a$, $\tau = 3\ln[a_{cr}(t)/a_{cr}(0)]$, $\mathcal{C}(g) = C(a,z)/a$, and $\mathcal{Z}(g) = a\,\dot{z}/(D[c_\infty - c_s(a)])$, Eqs. (2) and (4) become

$$\frac{du^3}{d\tau} = \gamma(u-1)\mathcal{C}(g) - u^3 \tag{5}$$

and

$$\frac{dg}{d\tau} = \frac{1}{3}\gamma(u^{-2}-u^{-3})[\mathcal{Z}(g) - g\mathcal{C}(g)] \tag{6}$$

with $\gamma \equiv (6D\Lambda c_0)/[d_t a_{cr}^3(t)]$. The value of γ describes the time dependence of the critical radius or the supersaturation, respectively. Since in the thermodynamic limit the latter is dominated by the bulk, the value of γ can be adopted from the LSW theory [12–14] as $\gamma = 27/4$, which implies $a_{cr} \propto t^{1/3}$.

A differential equation for the trajectory $g(u)$ for the late-stage growth of droplets follows from the ratio of (5) and (6),

$$\frac{dg}{du} = \frac{\gamma(u-1)[\mathcal{Z}(g) - g\mathcal{C}(g)]}{\gamma(u^2-u)\mathcal{C}(g) - u^4} \equiv F(u,g). \tag{7}$$

Numerical integration produces Figs. 1 and 2, where all trajectories run from the right to the left (i.e., $\dot{u} \leqslant 0$). The upper line ($g^{-1}=0$) of Fig. 1 represents the bulk behavior of the system discussed in the LSW theory [12–14]. A well-known result of this theory is that the source at $g^{-1}=0, u=3/2$ leads to a steady state droplet-size distribution $\varphi(\tau,u)$, which is insensitive to the initial conditions. For $u<3/2$ the function $\varphi(\tau,u)$ has the form

$$\varphi(\tau,u) = Ae^{-\tau}\frac{1}{-v(u)}\exp\left[\int_0^u \frac{du}{v(u)}\right] = Ae^{-\tau}\frac{3^4 e}{2^{5/3}}\frac{u^2\,\exp\left[\dfrac{-1}{1-2u/3}\right]}{(u+3)^{7/3}(3/2-u)^{11/3}} \tag{8}$$

with $v(u) \equiv du/d\tau$ and it vanishes for $u > 3/2$.

In Fig. 1 one can distinguish three regions of different physical behavior. In the left corner below the dotted line no trajectories are shown because the corresponding droplets on these trajectories would come out of the wall, which makes no sense. The region above the dotted and below the dashed line (including the trajectories running into the wall at $u > 1$) is fed from the volume ($g^{-1} \to 0$) with infinite initial values of the radii u. Also, for radii u larger than 3/2 there exist no droplets in the bulk. As a consequence no droplets do exist in the whole region which according to Fig. 2 corresponds to a layer of a thickness of about three critical radii at the wall. This means that in the late stage of the ripening process a depletion layer will grow at a rate $\propto t^{1/3}$. The dashed line in Fig. 1 represents the boundary trajectory belonging to the fixed point ($g^{-1}=0, u=3/2$). Above this boundary the flow along the trajectories can be characterized by the source strength of the fixed point, which is implicit in

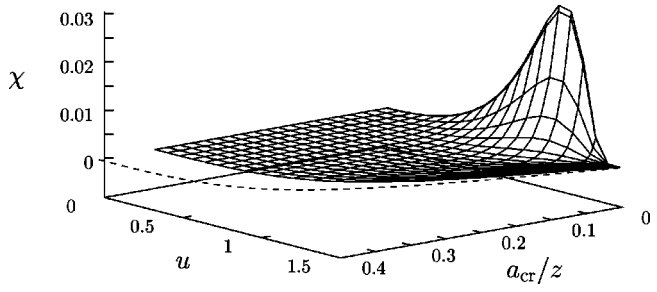

FIG. 3. Droplet-number distribution in the semi-infinite system.

Eq. (8). Integration of the continuity equation along the trajectories leads to the droplet-number distribution,

$$\varphi(\tau,u,z)=Ae^{-\tau}\frac{1}{-v_{g_1}(u)} \times\exp\left[\int_u^{3/2}du'\left(\left.\frac{\partial F(u',g)}{\partial g}\right|_{u',g(u',g_1)} -\left.\frac{\partial F(u',g)}{\partial g}\right|_{u',g(u',\infty)}\right) +\int_0^{3/2}du'\left(\frac{1}{v_\infty(u')}-\frac{1}{v_{g_1}(u')}\right) +\int_0^{u}du'\,\frac{1}{v_{g_1}(u')}\right]. \tag{9}$$

Here $g(u,g_1)$ are the trajectories parametrized by their minima $g_1\equiv g(u=1)$ and $v_{g_1}(u)$ means the velocity $du/d\tau$ on the trajectory g_1 at the radius u. The expression (9) has been evaluated numerically and the result for $\chi(u,z)\equiv A^{-1}e^{\tau}\varphi(\tau,u,z)$ is plotted in Fig. 3. Again the dashed line represents the boundary trajectory of the fixed point. The curve in the χ-u plane at $a_{\rm cr}/z=0$ displays the usual bulk distribution (8). Generally, Fig. 3 shows a smooth decrease in the droplet-number density from the bulk to the boundary trajectory of the fixed point.

In conclusion we offer a qualitative interpretation of the main results of the present paper. In a semi-infinite system with a dry boundary wall the droplets close to this wall grow slower than the droplets that are far away because the wall screens the diffusional flux into the droplet. In the thermodynamic limit the droplets far away from the wall reduce the supersaturation and drive the critical radius faster than the radius of a droplet close to the wall. A supercritical droplet that grows in the bulk approaches the wall in units of g because of its increasing radius, which leads to an impairment of its growth properties. The former supercritical droplet gets surpassed by the critical radius, becomes subcritical and vanishes before it can reach the wall. This is the mechanism that leads to the building up of the growing depletion zone close to the wall. Of course it would be interesting to see this effect in an experiment.

I thank R. Bausch and R. Blossey for various helpful discussions. This work was supported by the Deutsche Forschungsgemeinschaft under SFB 237 (Unordnung und große Fluktuationen).

[1] J. D. Gunton, P. S. Sahni, and M. San Miguel, *Phase Transitions and Critical Phenomena*, edited by C. Domb and J. L. Lebowitz (Academic, London, 1983), Vol. 8.
[2] K. Binder, Rep. Prog. Phys. **50**, 783 (1987).
[3] G. Brown, A. Chakrabarti, and J. F. Marko, Phys. Rev. E **50**, 1674 (1994).
[4] R. Bausch and R. Blossey, Phys. Rev. E **48**, 1131 (1993).
[5] R. Blossey, Int. J. Mod. Phys. B **9**, 3489 (1995).
[6] R. C. Ball and R. L. H. Essery, J. Phys.: Condens. Matter **2**, 10 303 (1990).
[7] P. Wiltzius and A. Cumming, Phys. Rev. Lett. **66**, 3000 (1991).
[8] S. M. Troian, Phys. Rev. Lett. **71**, 1399 (1993).
[9] G. Krausch, E. J. Kramer, F. S. Bates, J. F. Marko, G. Brown, and A. Chakrabarti, Macromolecules **27**, 6768 (1994).
[10] S. Puri and K. Binder, Phys. Rev. E **49**, 5359 (1994).
[11] H. Tanaka, J. Chem. Phys. **L103**, 2361 (1995).
[12] I. M. Lifshitz and V. V. Slyozov, J. Phys. Chem. Solids **19**, 35 (1961).
[13] L. D. Landau and E. M. Lifshitz, *Course of Theoretical Physics* (Pergamon, Oxford, 1981), Vol. 10.
[14] C. Wagner, Z. Elektrochem. **65**, 581 (1961).
[15] The electrostatics of two spheres can be calculated by iteration of the method of mirror-charges, see, e.g., F. Kottler in *Handbuch der Physik XII*, edited by H. Geiger (Springer, Berlin, 1927).
[16] R. Burghaus, Phys. Rev. E **54**, 6955 (1996).
[17] R. G. Picknett and R. Bexon, J. Colloid Interface Sci. **61**, 336 (1977).